



# Micron Scale Spatial Measurement of the O<sub>2</sub> Gradient Surrounding a Bacterial Biofilm in Real Time

Alexander D. Klementiev,<sup>a</sup> Zhaoyu Jin,<sup>d</sup> Marvin Whiteley<sup>a,b,c</sup>

<sup>a</sup>School of Biological Sciences, Georgia Institute of Technology, Atlanta, Georgia, USA

<sup>b</sup>Emory-Children's Cystic Fibrosis Center, Atlanta, Georgia, USA

<sup>c</sup>Center for Microbial Dynamics and Infection, Georgia Institute of Technology, Atlanta, Georgia, USA

<sup>d</sup>Center for Electrochemistry, Department of Chemistry, The University of Texas at Austin, Austin, Texas, USA

**ABSTRACT** Bacteria alter their local chemical environment through both consumption and the production of a variety of molecules, ultimately shaping the local ecology. Molecular oxygen (O<sub>2</sub>) is a key metabolite that affects the physiology and behavior of virtually all bacteria, and its consumption often results in O<sub>2</sub> gradients within sessile bacterial communities (biofilms). O<sub>2</sub> plays a critical role in several bacterial phenotypes, including antibiotic tolerance; however, our understanding of O<sub>2</sub> levels within and surrounding biofilms has been hampered by the difficulties in measuring O<sub>2</sub> levels in real-time for extended durations and at the micron scale. Here, we developed electrochemical methodology based on scanning electrochemical microscopy to quantify the O<sub>2</sub> gradients present above a *Pseudomonas aeruginosa* biofilm. These results reveal that a biofilm produces a hypoxic zone that extends hundreds of microns from the biofilm surface within minutes and that the biofilm consumes O<sub>2</sub> at a maximum rate. Treating the biofilm with levels of the antibiotic ciprofloxacin that kill 99% of the bacteria did not affect the O<sub>2</sub> gradient, indicating that the biofilm is highly resilient to antimicrobial treatment in regard to O<sub>2</sub> consumption.

**IMPORTANCE** O<sub>2</sub> is a fundamental environmental metabolite that affects all life on earth. While toxic to many microbes and obligately required by others, those that have appropriate physiological responses survive and can even benefit from various levels of O<sub>2</sub>, particularly in biofilm communities. Although most studies have focused on measuring O<sub>2</sub> within biofilms, little is known about O<sub>2</sub> gradients surrounding biofilms. Here, we developed electrochemical methodology based on scanning electrochemical microscopy to measure the O<sub>2</sub> gradients surrounding biofilms in real time on the micron scale. Our results reveal that *P. aeruginosa* biofilms produce a hypoxic zone that can extend hundreds of microns from the biofilm surface and that this gradient remains even after the addition of antibiotic concentrations that eradicated 99% of viable cells. Our results provide a high resolution of the O<sub>2</sub> gradients produced by *P. aeruginosa* biofilms and reveal sustained O<sub>2</sub> consumption in the presence of antibiotics.

**KEYWORDS** biofilm, oxygen, antibiotics, electrochemistry, *Pseudomonas aeruginosa*, antibiotic resistance

Molecular oxygen (O<sub>2</sub>) is one of the most important molecules dictating bacterial lifestyle and behavior. For organisms capable of tolerating O<sub>2</sub>, it can provide a means to remove excess electrons formed during metabolism. While general fundamentals of O<sub>2</sub> consumption are well established, the role of O<sub>2</sub> is complex in bacterial communities, including those associated with human infection, since O<sub>2</sub> levels vary tremendously based on the infection site and the host response (1–3). In addition,

**Citation** Klementiev AD, Jin Z, Whiteley M. 2020. Micron scale spatial measurement of the O<sub>2</sub> gradient surrounding a bacterial biofilm in real time. *mBio* 11:e02536-20. <https://doi.org/10.1128/mBio.02536-20>.

**Editor** Matthew R. Parsek, University of Washington

**Copyright** © 2020 Klementiev et al. This is an open-access article distributed under the terms of the [Creative Commons Attribution 4.0 International license](https://creativecommons.org/licenses/by/4.0/).

Address correspondence to Marvin Whiteley, [marvin.whiteley@biosci.gatech.edu](mailto:marvin.whiteley@biosci.gatech.edu).

This article is a direct contribution from Marvin Whiteley, a Fellow of the American Academy of Microbiology, who arranged for and secured reviews by Philip Stewart, Montana State University, and Dipankar Koley, Oregon State University.

**Received** 4 September 2020

**Accepted** 18 September 2020

**Published** 20 October 2020

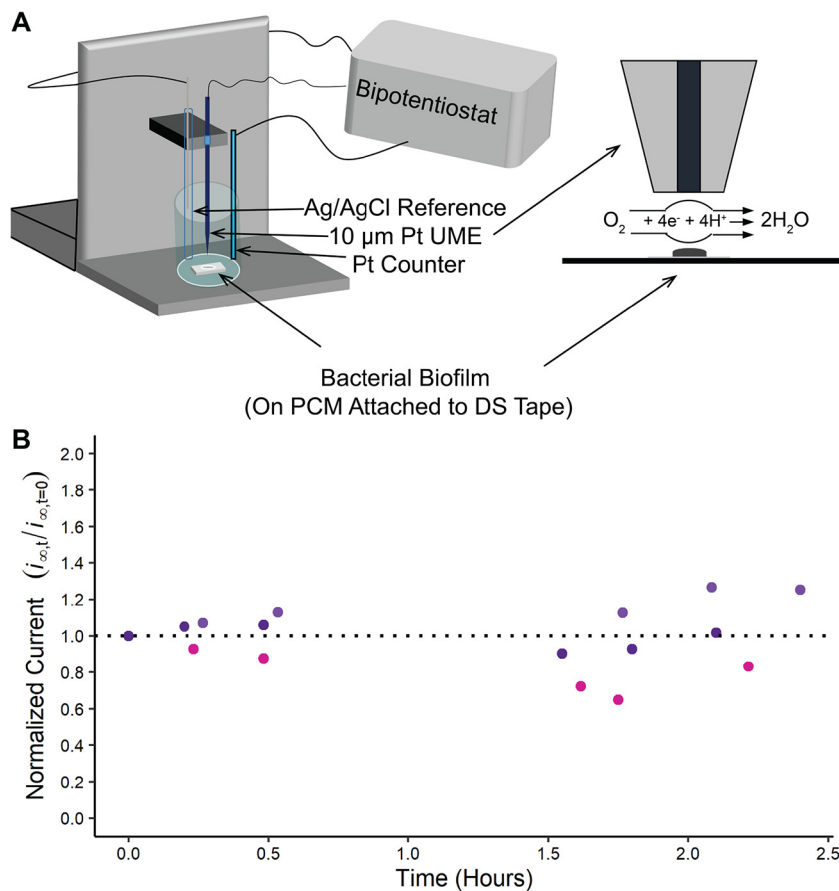


**FIG 1** Experimental system and SECM detection of the  $\text{O}_2$  gradient surrounding a *P. aeruginosa* biofilm. (A) Schematic of SECM setup for measurement of  $\text{O}_2$  gradient surrounding a *P. aeruginosa* biofilm (left), including a closeup of the SECM cell and  $\text{O}_2$  reduction reaction at the UME tip (right). (B) The platinized UME continuously monitors bulk  $\text{O}_2$  levels through measurement of tip current over several hours without loss of sensitivity. The y axis (ordinate) is the ratio of the tip current at each time point divided by the tip current at time zero. Each color represent biological replicates. PCM, polycarbonate membrane; DS, double-sided; UME, ultramicroelectrode.

bacteria in many infections grow as sessile communities called biofilms (4), and the three-dimensional structure of these communities can affect  $\text{O}_2$  levels throughout the biofilm.

Previous work has shown that  $\text{O}_2$  gradients within biofilms affect their biology (5, 6). This has prompted an examination of  $\text{O}_2$  levels within and surrounding biofilms. In particular, stagnant biofilms rapidly deplete  $\text{O}_2$  and waste material buildup occurs as a result of mass transport limitation at the surface of biofilms (7). Although it is clear that  $\text{O}_2$  levels are decreased within the biofilm, the levels immediately adjacent to the biofilm surface have not been thoroughly investigated in static biofilms, in part due to the difficulties in robustly measuring  $\text{O}_2$  with high spatial precision (5, 8–13). To address this gap in knowledge, we developed a system to spatially measure  $\text{O}_2$  levels above a microbial biofilm in real time at the micron scale. We chose the facultative anaerobe *Pseudomonas aeruginosa* strain PA14 for these studies since this opportunistic pathogen preferentially utilizes aerobic respiration (14), and its physiology and behavior are highly influenced by  $\text{O}_2$  availability (14, 15).

A significant challenge that was overcome is the inherent difficulty with continuously measuring  $\text{O}_2$  over extended time periods. To address this challenge, we developed a system using electrochemical methods to measure  $\text{O}_2$  in real-time with micron-scale spatial resolution (Fig. 1A).  $\text{O}_2$  can be detected electrochemically through a four-electron reduction on a platinum ultramicroelectrode (UME) (Fig. 1A) (16). How-

ever, platinum UMEs readily deactivate which leads to long wait times for O<sub>2</sub> current stabilization and sub-nA current (see Fig. S1 in the supplemental material). To address this challenge, we optimized a platinization protocol that coats the UME surface with platinum particles that actively reduce O<sub>2</sub> while avoiding severe changes in the geometry of the UME surface (see Fig. S2). Importantly, our platinum UMEs had a higher electroactive area and could continuously monitor O<sub>2</sub> levels over several hours without loss of sensitivity (Fig. 1B). This is especially important because the current measured in bulk was approximated to be 205 μM; since current measured is directly proportional to O<sub>2</sub> concentration, stability ensures accurate O<sub>2</sub> measurement despite each platinized UME used only once per experiment and having slightly variable degrees of platinization or size after polishing.

We next sought to measure O<sub>2</sub> levels surrounding a *P. aeruginosa* biofilm using scanning electrochemical microscopy (SECM). The *P. aeruginosa* strain chosen for this work (*fliC9::MrT7*) (17) has an inactivated flagellar motor protein, rendering the strain unable to leave the biofilm via swimming motility. Biofilms of the *P. aeruginosa* *fliC* mutant were formed on polycarbonate membranes as previously described for electrochemical studies (18). Membrane biofilms were grown for 8 h on Todd Hewitt broth (THB) agar, yielding an ~3-mm-diameter nascent biofilm containing ~4 × 10<sup>7</sup> bacteria (see Fig. S3). These biofilms contain fewer cells than those used in previous studies (5, 8) focused on O<sub>2</sub> consumption to better mimic biofilms observed in human infections. After formation, the membrane containing the biofilm was removed from the agar plate and attached to the bottom of a glass vial using double-sided tape and covered with ~5 ml of morpholinepropanesulfonic acid (MOPS)-glucose minimal medium.

To measure O<sub>2</sub> levels above the biofilm, a 10-μm-diameter platinized UME was approached to 40 μm above the biofilm surface using ferrocenyl methyl trimethylammonium (FcMTMA<sup>+</sup>; the toxicity and stability are assessed in Text S1 in the supplemental material) as the redox mediator (Fig. S4 and S5) using SECM (19). The UME tip was then poised at -0.5 V (O<sub>2</sub> reduction potential), with a wait time of 5 min; afterward, the UME was retracted at 6 μm/s while continually measuring O<sub>2</sub> until bulk O<sub>2</sub> levels were detected, ~1,400 μm above the biofilm surface (the O<sub>2</sub> gradient calculations are detailed in Text S1). The O<sub>2</sub> levels above the biofilm resembled a sigmoidal curve with no O<sub>2</sub> detectable until ~200 μm above the biofilm (Fig. 2A; see also Fig. S6). Assuming a 10-pA minimal background current, the detection limit of the UME is ~1 μM.

For comparison, we created an O<sub>2</sub> gradient without a biofilm using a platinum electrode the same size as the biofilm as the SECM substrate. The 3-mm platinum electrode was held at three potentials (0.1, 0, and -0.5 V versus Ag/AgCl) for 5 min, and then the O<sub>2</sub> gradient was measured as described for the biofilm (detailed in Text S1). The biofilm O<sub>2</sub> gradient was similar to the -0.5 V poised electrode gradient, which is the potential at which O<sub>2</sub> reduction is mass transport limited at the surface of the electrode. The biofilm O<sub>2</sub> gradient was distinct from the other potentials at which O<sub>2</sub> was being consumed at a submaximal rate (i.e., limited in part by kinetics and not predominantly by mass transport). Using Comsol Multiphysics to digitally simulate O<sub>2</sub> consumption (Fig. 2B; see also Fig. S7), we approximated the flux of O<sub>2</sub> at the surface of the biofilm to be 8.2 × 10<sup>-7</sup> mol/cm<sup>2</sup>/s (detailed in Text S1). Assuming each cell has a dimension of 1.5 μm × 0.8 μm, 9.8 × 10<sup>-15</sup> mol/s O<sub>2</sub> or 5.9 × 10<sup>9</sup> molecules of O<sub>2</sub> per second were consumed by each bacterium. Collectively, these results reveal that *P. aeruginosa* biofilms produce a hypoxic zone that can extend hundreds of microns from the biofilm surface within minutes, and the biofilm consumes O<sub>2</sub> at a maximum rate.

To assess the effect of antibiotic treatment on biofilm O<sub>2</sub> consumption, we treated our biofilms with 400 times the MIC of the antibiotic ciprofloxacin (40 μg/ml) and then measured the O<sub>2</sub> gradient above the biofilm. We first confirmed that ciprofloxacin does not interfere with the electrochemical signal for O<sub>2</sub> quantification (Fig. S8; see also Text S1). Ciprofloxacin treatment of the biofilm was performed by initially adding 20 μg/ml ciprofloxacin and measuring the O<sub>2</sub> response 1.5 h after submersion in MOPS-glucose (Fig. 2C). After we observed no immediate change in signal, we treated the biofilm with another 20 μg/ml. After addition of the second dose of ciprofloxacin, the O<sub>2</sub> gradient

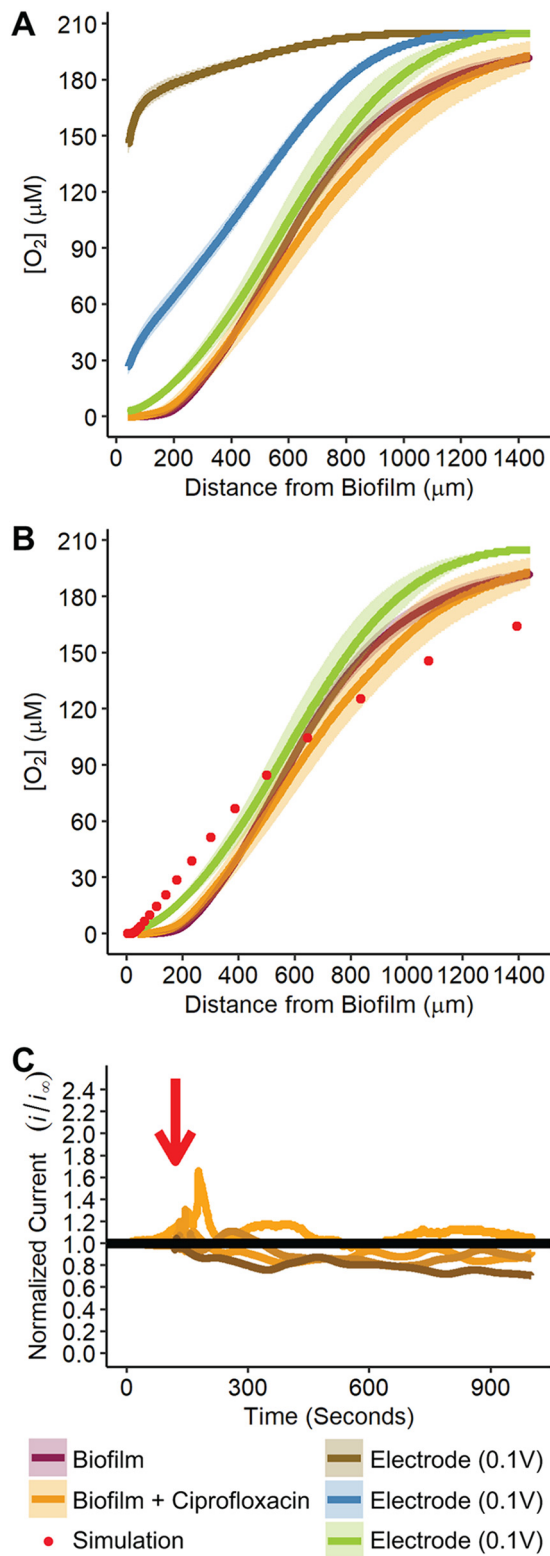


**FIG 2** *P. aeruginosa* rapidly produce  $O_2$  gradients that are resilient to antibiotic treatment. (A)  $O_2$  gradients above the surface of *P. aeruginosa* biofilms, *P. aeruginosa* biofilms treated with ciprofloxacin, and for reference a 3-mm platinum electrode poised at 0, 0.1, and  $-0.5$  V versus Ag/AgCl (different electrode potentials correspond to various  $O_2$  consumption rates).  $n = 4$  biological replicates for Electrode 0.1 V, Electrode 0 V, Electrode  $-0.5$  V, and Biofilm + Ciprofloxacin, and  $n = 16$  biological replicates for biofilm. For all  $O_2$  gradients, shading represents one standard deviation from the mean (solid line). (B) Digital simulation (red circles) to estimate  $O_2$  consumption rates of the biofilm. The model was solved by Comsol Multiphysics (5.3a; COMSOL, Inc., Burlington, MA) using the electrochemical

(Continued on next page)

was measured for 50 min with no observable change in the O<sub>2</sub> gradient, a total of 1 h and 35 min after ciprofloxacin was first added. Despite the fact that addition of ciprofloxacin reduced the number of viable bacteria in the biofilm by 100-fold to  $\sim 2.4 \times 10^5$  bacteria, there was no change in the O<sub>2</sub> gradient or O<sub>2</sub> consumption rates (Fig. 2A and B).

While prior work has primarily measured bulk O<sub>2</sub> at the biofilm/air interface, we show that, in contrast, at a stagnant biofilm/liquid interface a hypoxic region forms several hundred microns above the biofilm surface. Containing only  $\sim 4 \times 10^7$  bacteria, our biofilms consumed O<sub>2</sub> at maximum rates and continued to do so despite 99% killing by ciprofloxacin. These data corroborate similar findings that bulk respiratory activity and carbon consumption persists despite antibiotic exposure (20, 21). Given this high O<sub>2</sub> consumption rate and the observation that biofilms of this size exist in human implant/catheter infections (22), we propose that biofilms are capable of rapidly depleting local O<sub>2</sub> in chronic infections even during antibiotic challenge. Ultimately, the experimental system developed in this work provides a valuable framework for studying biofilm O<sub>2</sub> consumption.

## MATERIALS AND METHODS

**Instrumentation.** Initial electrochemistry experiments were performed using a BioLogic SECM (model M470). Biofilm experiments measuring O<sub>2</sub> gradients by scanning distances were done using a CHI model 920D scanning electrochemical microscope (CH Instruments). For all experiments, a three-electrode setup was used. This consisted of a 10- $\mu$ m-diameter platinum UME (working electrode), Ag|AgCl|Saturated KCl (reference electrode to which all potentials are referred to in all experiments), and platinum wire (counter electrode). An in-depth protocol for UME fabrication may be found elsewhere (19).

**Ultramicroelectrode fabrication and SECM cell setup.** An in-depth protocol for UME fabrication may be found elsewhere (19). Briefly, platinum (99.9% purity) wire, 10- $\mu$ m diameter, temper: hard (Goodfellow Metals, Cambridge, United Kingdom; product PT005107) was used for the preparation of the SECM UME tip. The metal wire was heat sealed with a heating coil under vacuum in a glass capillary. The tip was sharpened to an RG of  $\sim 10$ , where RG is the ratio of the glass diameter to wire diameter. Prior to electrochemical experiments, UMEs were sonicated in a water bath for 30 s. Platinization significantly alters the surface and UMEs were seldom repolished and replatinized for reuse.

**Bacterial strain culture and preparation.** *P. aeruginosa* (PA14) *fliC9::MrT7* mutant was obtained from a PA14 nonredundant transposon insertion mutant set (<http://ausubellab.mgh.harvard.edu/cgi-bin/pa14/home.cgi>) (17). Biofilms were grown in THB agar for 8 h at 37°C, at which point an  $\sim 3$ -mm-diameter biofilm formed before transfer to the SECM cell. All SECM experiments were performed using MOPS minimal media (23) containing 20 mM glucose. CFU were enumerated at the end of experimentation by removing media above the biofilm, substantially vortexing the biofilm off the polycarbonate membrane, and plating on THB agar plates overnight at 37°C.

**Platinizing UMEs.** Handmade 10  $\mu$ m platinum UMEs (as described above) were sonicated in water, acetone, and water. A modified protocol for platinizing UMEs was used that may be found elsewhere (24) with an adjusted recipe for the platinization solution containing 0.250 ml of H<sub>2</sub>PtCl<sub>6</sub> and 0.4 mg of Pb(NO<sub>3</sub>)<sub>2</sub> up to a final volume of 7.36 ml in 1 $\times$  phosphate-buffered saline (pH 7.4). Geometric and electroactive effects on the UME surface resulting from platinization were measured to confirm the stability and reproducibility of platinization. An in-depth review of platinizing electrodes can be found elsewhere (25).

**Measuring O<sub>2</sub>.** PA14 *tn::fliC* biofilms were grown as described above. After 8 h growth, the polycarbonate membrane was removed and attached to the bottom of a custom glass vial using double sided tape. UMEs were cycled in platinizing solution (same as above) from 0.2 V to  $-0.3$  V versus Ag/AgCl at 100 mV/s until the maximum limiting current increased  $\sim 1.2\times$  for FcMTMA<sup>+</sup> oxidation (the synthesis is detailed in Text S1). After platinization and ensuring proper geometric area of the UMEs, 1 mM FcMTMA<sup>+</sup> was added to MOPS-glucose media, and approximately 5 ml was added to the vial containing the biofilm. A three-electrode setup using a platinum wire counter, and Ag/AgCl reference electrodes were connected. Platinized UMEs were precisely positioned with micron-scale accuracy using SECM. SECM

### FIG 2 Legend (Continued)

analysis module in two-dimensional axial symmetry using stationary conditions with a parametric sweep of the “d” or distance between UME tip and substrate (Fig. S5, and detailed in Text S1). (C) Changes in O<sub>2</sub> concentration 600  $\mu$ m above a biofilm measured as a response to ciprofloxacin treatment. At 120 s, the first dose of 20  $\mu$ g/ml ciprofloxacin was added (designated by red arrow). Each line represents a biological replicate. The y axis (ordinate) is the ratio of the tip current at each time point divided by current measured before ciprofloxacin addition (i.e., a value of 1 indicates no change in current after ciprofloxacin addition). There were changes immediately after ciprofloxacin addition (peaks at red arrow), likely a result of the mixing caused by addition of ciprofloxacin to the growth media above the biofilm. Importantly, the current quickly stabilized.

positions UMEs at defined distances from the biofilm surface using an electroactive mediator while observing tip current changes as a function of distance. For this work, we chose the electroactive mediator FcMTMA<sup>+</sup> since it is neither consumed by nor is toxic to *P. aeruginosa*. UMEs were poised at 0.5 V to oxidize FcMTMA<sup>+</sup>, approached within ~40 μm above the surface (within the hindered diffusion region corresponding to a decrease in signal to ~95% limiting current), and then poised at -0.5 V and retracted at 6 μm/s to measure O<sub>2</sub> gradients. For antibiotic chronoamperometry curves, UMEs were positioned first approximately 600 μm for the first addition of ciprofloxacin or control, approximately 1 h and 30 min elapsed after MOPS-glucose was added over the biofilm. Ciprofloxacin was added slowly during this time at ~7.5 mm above the biofilm, and the stage was attached to the vial containing the biofilm was rotated 10 times in a circular motion immediately after addition. The UME was then approached approximately 300 μm above the biofilm for the second addition of ciprofloxacin, approximately 2 h elapsed after MOPS-glucose was added over the biofilm. Ciprofloxacin or control was then added quickly at ~7.5 mm above the biofilm. For both additions, a 2-min window was given before antibiotics were added to the media and current was measured for a minimum of 1,000 s in total. O<sub>2</sub> concentration gradients were immediately measured in triplicate during each biological replicate after the second addition of antibiotics to determine the O<sub>2</sub> consumption rates.

## SUPPLEMENTAL MATERIAL

Supplemental material is available online only.

**TEXT S1**, PDF file, 0.2 MB.

**FIG S1**, PDF file, 0.1 MB.

**FIG S2**, PDF file, 0.1 MB.

**FIG S3**, PDF file, 0.04 MB.

**FIG S4**, PDF file, 0.1 MB.

**FIG S5**, PDF file, 0.3 MB.

**FIG S6**, PDF file, 0.2 MB.

**FIG S7**, PDF file, 0.03 MB.

**FIG S8**, PDF file, 0.2 MB.

## ACKNOWLEDGMENTS

We thank Cynthia Zoski, Allen Bard, Cesar Ortiz, Tianhan Kai, Min Zhou, and the Whiteley lab for valuable discussions. We also thank Bryan W. Davies, UT Austin, for providing lab space.

This study was supported by National Institutes of Health grants R01GM116547 (to M.W.), Cystic Fibrosis Foundation grants WHITEL19P0 and WHITEL16G0 (to M.W.), and 1F31DE029415-01 (to A.D.K.). M.W. is a Burroughs Wellcome Investigator in the Pathogenesis of Infectious Disease.

## REFERENCES

- Mettraux G, A Gusberti F, Graf H. 1984. Oxygen tension (pO<sub>2</sub>) in untreated human periodontal pockets. *J Periodontol* 55:516–521. <https://doi.org/10.1902/jop.1984.55.9.516>.
- Hopf HW, Hunt TK, West JM, Blomquist P, Goodson WH, Jensen JA, Jonsson K, Paty PB, Rabkin JM, Upton RA, von Smitten K, Whitney JD. 1997. Wound tissue oxygen tension predicts the risk of wound infection in surgical patients. *Arch Surg* 132:997–1004. <https://doi.org/10.1001/archsurg.1997.01430330063010>.
- Kalani M, Brismar K, Fagrell B, Ostergren J, Jörneskog G. 1999. Transcutaneous oxygen tension and toe blood pressure as predictors for outcome of diabetic foot ulcers. *Diabetes Care* 22:147–151. <https://doi.org/10.2337/diacare.22.1.147>.
- James GA, Swogger E, Wolcott R, Pulcini E, Secor P, Sestrich J, Costerton JW, Stewart PS. 2008. Biofilms in chronic wounds. *Wound Repair Regen* 16:37–44. <https://doi.org/10.1111/j.1524-475X.2007.00321.x>.
- Walters MC, III, Roe F, Bugnicourt A, Franklin MJ, Stewart PS. 2003. Contributions of antibiotic penetration, oxygen limitation, and low metabolic activity to tolerance of *Pseudomonas aeruginosa* biofilms to ciprofloxacin and tobramycin. *Antimicrob Agents Chemother* 47:317–323. <https://doi.org/10.1128/aac.47.1.317-323.2003>.
- Wessel AK, Arshad TA, Fitzpatrick M, Connell JL, Bonnez RT, Shear JB, Whiteley M. 2014. Oxygen limitation within a bacterial aggregate. *mBio* 5:e00992. <https://doi.org/10.1128/mBio.00992-14>.
- Stewart PS. 2012. Mini-review: convection around biofilms. *Biofouling* 28:187–198. <https://doi.org/10.1080/08927014.2012.662641>.
- Dietrich LEP, Okegbe C, Price-Whelan A, Sakhtah H, Hunter RC, Newman DK. 2013. Bacterial community morphogenesis is intimately linked to the intracellular redox state. *J Bacteriol* 195:1371–1380. <https://doi.org/10.1128/JB.02273-12>.
- Ahimou F, Semmens MJ, Haugstad G, Novak PJ. 2007. Effect of protein, polysaccharide, and oxygen concentration profiles on biofilm cohesiveness. *Appl Environ Microbiol* 73:2905–2910. <https://doi.org/10.1128/AEM.02420-06>.
- Kühl M, Jørgensen BB. 1992. Microsensor measurements of sulfate reduction and sulfide oxidation in compact microbial communities of aerobic biofilms. *Appl Environ Microbiol* 58:1164–1174. <https://doi.org/10.1128/AEM.58.4.1164-1174.1992>.
- de Beer D, Stoodley P, Roe F, Lewandowski Z. 1994. Effects of biofilm structures on oxygen distribution and mass transport. *Biotechnol Bioeng* 43:1131–1138. <https://doi.org/10.1002/bit.260431118>.
- Rasmussen K, Lewandowski Z. 1998. Microelectrode measurements of local mass transport rates in heterogeneous biofilms. *Biotechnol Bioeng* 59:302–309. [https://doi.org/10.1002/\(SICI\)1097-0290\(19980805\)59:3<302::AID-BIT6>3.0.CO;2-F](https://doi.org/10.1002/(SICI)1097-0290(19980805)59:3<302::AID-BIT6>3.0.CO;2-F).
- Staal M, Borisov SM, Rickelt LF, Klimant I, Kühl M. 2011. Ultrabright planar optodes for luminescence life-time based microscopic imaging of O<sub>2</sub> dynamics in biofilms. *J Microbiol Methods* 85:67–74. <https://doi.org/10.1016/j.mimet.2011.01.021>.
- Alvarez-Ortega C, Harwood CS. 2007. Responses of *Pseudomonas aeruginosa* to low oxygen indicate that growth in the cystic fibrosis lung is by aerobic respiration. *Mol Microbiol* 65:153–165. <https://doi.org/10.1111/j.1365-2958.2007.05772.x>.

15. Schertzer JW, Brown SA, Whiteley M. 2010. Oxygen levels rapidly modulate *Pseudomonas aeruginosa* social behaviours via substrate limitation of PqsH. *Mol Microbiol* 77:1527–1538. <https://doi.org/10.1111/j.1365-2958.2010.07303.x>.
16. Sánchez-Sánchez CM, Bard AJ. 2009. Hydrogen peroxide production in the oxygen reduction reaction at different electrocatalysts as quantified by scanning electrochemical microscopy. *Anal Chem* 81:8094–8100. <https://doi.org/10.1021/ac901291v>.
17. Liberati NT, Urbach JM, Miyata S, Lee DG, Drenkard E, Wu G, Villanueva J, Wei T, Ausubel FM. 2006. An ordered, nonredundant library of *Pseudomonas aeruginosa* strain PA14 transposon insertion mutants. *Proc Natl Acad Sci U S A* 103:2833–2838. <https://doi.org/10.1073/pnas.0511100103>.
18. Liu X, Ramsey MM, Chen X, Koley D, Whiteley M, Bard AJ. 2011. Real-time mapping of a hydrogen peroxide concentration profile across a polymicrobial bacterial biofilm using scanning electrochemical microscopy. *Proc Natl Acad Sci U S A* 108:2668–2673. <https://doi.org/10.1073/pnas.1018391108>.
19. Bard AJ, Mirkin MV. 2012. *Scanning electrochemical microscopy*, 2nd ed. Taylor & Francis, Abingdon-on-Thames, UK.
20. Stewart PS, White B, Boegli L, Hamerly T, Williamson KS, Franklin MJ, Bothner B, James GA, Fisher S, Vital-Lopez FG, Wallqvist A. 2019. Conceptual model of biofilm antibiotic tolerance that integrates phenomena of diffusion, metabolism, gene expression, and physiology. *J Bacteriol* 201:e00307-19. <https://doi.org/10.1128/JB.00307-19>.
21. Simkins JW, Stewart PS, Codd SL, Seymour JD. 2019. Non-invasive imaging of oxygen concentration in a complex *in vitro* biofilm infection model using (19) F MRI: persistence of an oxygen sink despite prolonged antibiotic therapy. *Magn Reson Med* 82:2248–2256. <https://doi.org/10.1002/mrm.27888>.
22. Bjarnsholt T, Alhede M, Alhede M, Eickhardt-Sørensen SR, Moser C, Kühl M, Jensen PØ, Høiby N. 2013. The *in vivo* biofilm. *Trends Microbiol* 21:466–474. <https://doi.org/10.1016/j.tim.2013.06.002>.
23. Palmer KL, Mashburn LM, Singh PK, Whiteley M. 2005. Cystic fibrosis sputum supports growth and cues key aspects of *Pseudomonas aeruginosa* physiology. *J Bacteriol* 187:5267–5277. <https://doi.org/10.1128/JB.187.15.5267-5277.2005>.
24. Li Y, Sella C, Lemaitre F, Guille Collignon M, Thouin L, Amatore C. 2013. Highly sensitive platinum-black coated platinum electrodes for electrochemical detection of hydrogen peroxide and nitrite in microchannel. *Electroanalysis* 25:895–902. <https://doi.org/10.1002/elan.201200456>.
25. Feltham AM, Spiro M. 1971. Platinized platinum electrodes. *Chem Rev* 71:177–193. <https://doi.org/10.1021/cr60270a002>.